**Universität Stuttgart**
*Institut für Energiespeicherung*
Professor Dr. André Thess

**Deutsches Zentrum für Luft- und Raumfahrt**
**Institut für Technische Thermodynamik**

**Student research paper**

# Implementation and Analysis of a Rolling Horizon Approach for the Energy System Model REMix

submitted by Sebastian Schreck
Matr.-Nr.: 2733207

Start date: 01.04.2016
Submission date: 28.07.2016

Supervisors:
Professor Dr. André Thess
M.Sc. Karl-Kiên Cao
Dipl.-Wi.-Ing. Felix Cebulla

# Decleration/Erklärung

I hereby certify that this research work has been composed by myself, and describes my own work, unless otherwise acknowledged in the text. All references and verbatim extracts have been quoted, and all resources have been specifically acknowledged. It has not been submitted to any previous application for a degree.

Ich versichere hiermit, dass ich diese Forschungsarbeit selbstständig durchgeführt und verfasst habe und, dass ich keine anderen als die angegebenen Quellen und Hilfsmittel benutzt habe. Die Arbeit ist weder veröffentlicht worden, noch hat sie in gleicher oder ähnlicher Form einer anderen Prüfungsbehörde vorgelegen. Weiterhin versichere ich, dass das elektronische Exemplar mit den anderen Exemplaren übereinstimmt.

Ort Datum Unterschrift

# Abstract/Kurzfassung

## Abstract

As energy system analysis faces increasingly complex research questions, energy system models like REMix (Renewable Energy Mix) deal with difficulties regarding the solvability of these models in a reasonable time. This thesis applies a rolling-horizon approach to REMix with the aim of a reduction in computational time while maintaining the key modeling features. In order to deal with the issue of modeling time-integral constraints like seasonal storage, an approach which uses overlapping time periods as well as a temporal-hierarchical methodology are presented and compared using a reference model. Through the application of a parameter study, the optimal configuration, i.e. number of intervals and overlap-sizing, of the rolling-horizon approach is determined for the reference model. The results show that a decrease in computational time of about 35% can be achieved using the developed temporal-hierarchical approach without a significant reduction of the modeling features.

## Kurzfassung

Durch die fortlaufend steigende Komplexität der Fragestellungen in der Energiesystemanalyse, stoßen Energiesystemmodelle wie REMix (Renewable Energy Mix) bezogen auf vertretbare Rechenzeiten an ihre Grenzen. Die vorliegende Forschungsarbeit wendet den Ansatz der rollierenden Einsatzplanung, mit dem Ziel einer Rechenzeitreduzierung unter Beibehaltung der essenziellen Modellierungsmerkmale, auf REMix an. Um der Herausforderung der Modellierung zeitintegraler Nebenbedingungen wie saisonaler Speicher entgegen zu treten, werden zwei Ansätze entwickelt und angewandt. Einerseits die Verwendung von überlappenden Zeitperioden und zum Anderen ein zeitlich-hierarchischer Ansatz. Weiterhin wird durch eine Parameterstudie die optimale Konfiguration der Ansätze untersucht indem verschiedene Intervallanzahlen mit unterschiedlichen überlappenden Zeitperioden kombiniert werden. Die Auswertung der Ergebnisse zeigt, dass durch die Anwendung der entwickelten Ansätze eine Rechenzeitreduzierung von bis zu 35%, ohne einen wesentlichen Verlust an Modellierungsgenauigkeit, erreicht werden kann.

# Contents

# List of Figures

# List of Tables

# 1. Introduction

## 1.1. Motivation

Driven by the aim of a sustainable, secure and affordable energy supply, the European energy system is currently experiencing a process of transformation. The liberalization and decentralization of the energy economy as well as the increasing expansion of renewable energies lead to a growing complexity of this system. To integrate intermittent renewable energies into the energy network, the system has to be expanded by balancing measures. Resulting political, technical and economic decisions regarding the future development of the energy system can be supported by quantitative energy system models like REMix [1].

REMix (Renewable Energy Mix for Sustainable Electricity Supply) is based on a linear, bottom-up optimization with a high temporal and spatial resolution, as well as a growing number of technologies. Flexibility options such as grid power transmission and grid expansion, storage systems or demand-side management further increase the model complexity and size. This leads to a rising effort in solving the associated linear optimization problems. System analysis of energy systems needs to address a wide range of research questions and thus, a big number of different models with growing complexity need to be solved. Furthermore, additional expansions of the model are planned for the future. As the computation of the model can reach non reasonable time and memory usage, options to decrease the mentioned have to be applied. Among the possibility of model reduction (e.g. lower temporal resolution or node aggregation) or decomposition approaches, the model can also be solved serially maintaining high resolution and complexity. This can be achieved by a rolling-horizon (RH) approach which splits the temporal model horizon into segments solving them iteratively. In contrast to a perfect-foresight annual optimization the problem size of each segment is reduced and thus a reduction of the mathematical complexity is achieved. Therefore, the objective of the present work is to apply a RH approach to REMix and analyze its effects.

## 1.2. Research question

The RH approach has been successfully applied to different kinds of energy system models mainly in the context of small microgrids and MILP (Mixed-Integer-Linear-Programming) ([2],[3],[4]). There are two main aims of the implementation in these kinds of models. On the one hand, reducing computational time by decreasing the number of integer variables in a model. On the other hand, taking into account the uncertainty of energy demand and renewable energy production using a rolling forecast. A massive decrease of computational time ranging from 10 to 100 times could be achieved in these models [2].

As the mentioned models are focused on dispatch and unit commitment problems (see [5]) in the context of small energy systems, their structure differs to the structure of REMix. Thus the following research questions have to be considered in the context of a large scale, spatially and temporally highly dissolved linear optimization model including optimal dispatch and capacity expansion:

1. What typical challenges occur in the implementation of a rolling-horizon approach?
2. Is a rolling-horizon approach suitable to reduce computational time?
3. Which configuration (e.g. sizing of the time segments) of the rolling-horizon approach delivers the best results?
4. How can a rolling-horizon approach be improved to reduce the error compared to the exact solution?

## 1.3. Structure of the thesis

The presented work is divided into 5 chapters. First, chapter 2 provides background information on the structure of REMix as well as an overview on acceleration possibilities for energy system models. Also, fundamental aspects and challenges regarding the design of a RH approach are described.

Chapter 3 addresses the method of implementing a rolling-horizon approach. At first, a test model is developed to identify the needed model adaptions. Using that knowledge, the rolling-horizon approach is implemented in REMix as a next step. To improve the quality of the rolling-horizon approach, a hierarchical heuristic focusing on temporal scaling is developed which enhances the behavior of seasonal storage, capacity expansion and time-integral restrictions. Besides, relevant indicators for the evaluation are determined in this chapter.

The results are analyzed and evaluated in chapter 4. This chapter focuses on the answer of research questions 2 and 3. Therefore the test model, a rolling-horizon approach for a dispatch model and an improved rolling-horizon approach are evaluated.

The last chapter summarizes and evaluates the results. Possible improvements of the rolling-horizon approach are discussed.

# 2. Background

## 2.1. Energy system model REMix

The energy system model REMix, developed at the German Aerospace Center (DLR), is a linear bottom–up–model. REMix uses the General Algebraic Modeling System (GAMS [6]) as a modeling language for mathematical optimization. The prevalent method in energy system modeling, linear optimization, is used to calculate the least-cost system configuration and operation using perfect foresight. An in-depth description of the model's structure and capability it can be found in [1] and [7]. However, to provide a better understanding of the functionality of REMix, the linear objective function of the problem is presented below:

$$\sum_{\tau,y}\left(c_{invest}(\tau,y)+\sum_{t}c_{operation}(\tau,y,t)\right)\rightarrow min, \tag{2.1}$$

$$\begin{aligned}&\forall\,\tau\,\epsilon\,TEC\\&\forall\,y\,\epsilon\,Y\\&\forall\,t\,\epsilon\,T\end{aligned}$$

Where $TEC$ describes the technologies used in the model, $T$ the time intervals contained by $y$, which defines the years considered for the calculation. In the following course of the work, the term dispatch is being used in relationship with $c_{operation}(\tau,y,t)$ of the objective function and respectively the term $c_{invest}(\tau,y)$ is being associated with capacity expansion.

Some specific features of REMix, necessary for the understanding of this work, are:

- A high resolution of the inputdata (e.g. renewable energy resources)
- The multi-sectoral approach providing electricity for the power, heat and transport sector
- Ability to model balancing measures like short-term storage systems in hourly resolution

Figure 2.1 describes the schematic structure of REMix. On the basis of the input-data, the hourly demand and renewable energy supply is calculated by the Energy Data Analysis Tool (EnDAT).

Combined with the technology and sceneraio input, the cost-minimized energy supply is calculated by the Energy System Optimization Model (OptiMo).

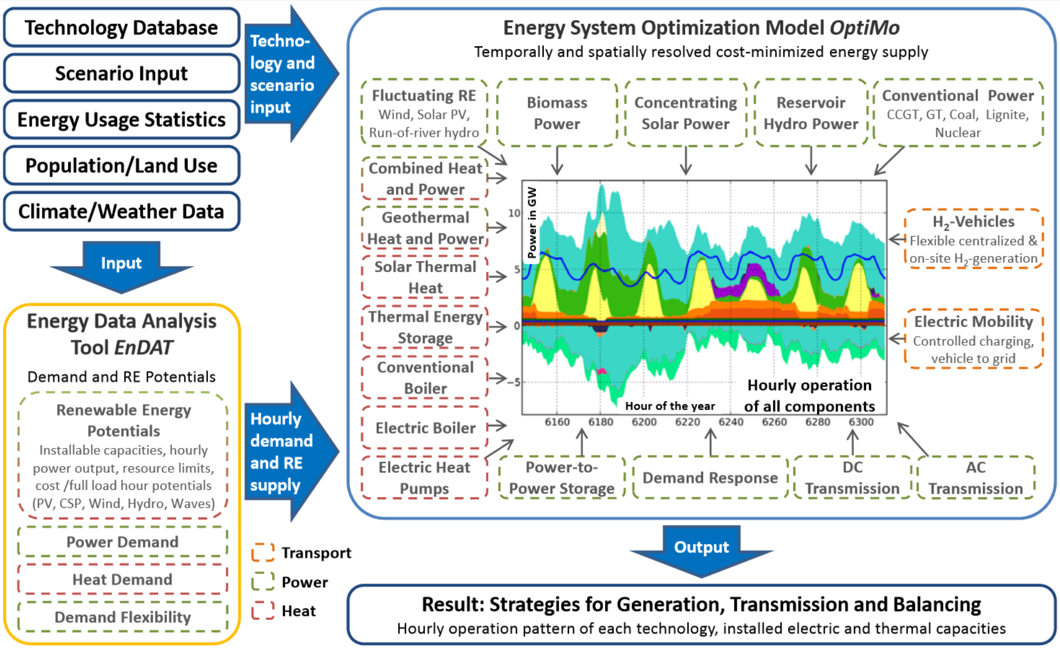

Figure 2.1.: Schematic description of the energy system model REMix [7]

As the rolling-horizon (RH) approach only finds an application in OptiMo, further remarks are referring to OptiMo. Figure 2.1 shows that OptiMo is composed of many different technology modules associated to different sectors. Using OptiMo as a tool for energy system analysis, it is sometimes necessary to consider a great number of modules, as well as a high temporal (typically 8760 time-steps for a year) and spatial resolution. Typical research questions for example include the analysis of the influence of short-term storage on transmission expansion in Europe. The computational time of the mentioned typical models remain within a range of several days. It is obvious that the calculation of a linear optimization problem with the mentioned requirements or even a higher level of detail, can lead to high computational times. Also, technologies like storage connect every single time step of the optimization horizon. That issue again makes the optimization problem harder to solve, because it generates equations with a huge amount of variables. Hence the RH approach addresses those problems by splitting the horizon into small segments.

## 2.2. Acceleration strategies for energy system models

Since there are several possibilities to accelerate the computation of energy system models, this chapter tries to classify the rolling–horizon approach in the context of different acceleration strategies. In general, there are two main approaches to achieve an acceleration of energy system models. First, by an adjustment and a parametrization of the used algorithms. Second, by changing the problem formulation. Since the RH approach can be seen as an adjusted problem formulation, only this kind of acceleration strategy is regarded. The following figure gives an overview of possible problem formulations with the aim of accelerating energy system models.

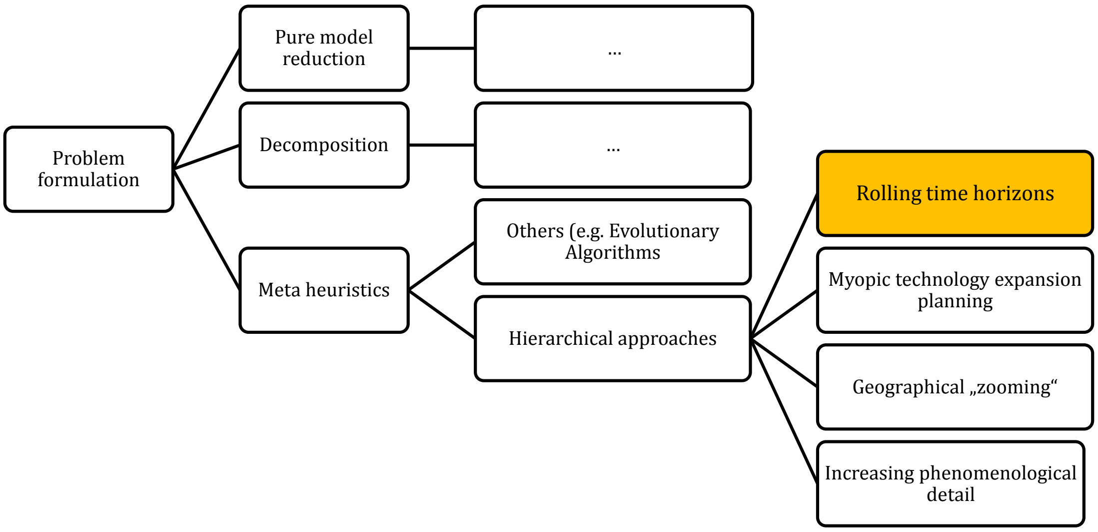

Figure 2.2.: Overview of possible problem formulations [8]

Pure model reduction can be used to simplify the model in an easy way. This can be achieved by reducing the number of technologies or using bigger time steps in the formulation of the optimization problem. Decomposition (e.g. Benders Decomposition [9]) uses the approach of dividing the problem into a master- and a sub-problem solving them iteratively. The RH approach can be classified in the category of meta-heuristics, since it is not guaranteed that the exact solution of the optimization problem is achieved. Another characteristic of the rolling-horizon approach is the segmentation of the original linear program into sub-problems. Problem formulations of the sub-category hierarchical approaches in figure 2.2 have in common that they solve the problem iteratively by using solution parts of the preceding linear program.

## 2.3. Rolling horizon optimization for energy system models

As mentioned in chapter 1.2, the rolling-horizon approach has been applied to many different energy system models. The following chapter gives an overview of the functional principle and difficulties using rolling-horizon in these models. Besides, important terms used in this work are defined.

### Terminology and fundamental principle

Instead of calculating an optimization problem (with the typical time horizon of one year) under perfect foresight, the problem is split into $I$ intervals with the respective interval-size $T_{interval}$. Starting from the first hour of the overall optimization horizon ($T$), the $I$ intervals are solved successively. After solving the optimization problem of an interval, values of time dependent variables are passed on to the following interval. To avoid an unrealistic behavior of technologies like seasonal storage, $T_{interval}$ can consists of a foresight-horizon ($T_{overlap}$) reaching into the following interval. Therefore $T_{interval}$ is divided into $T_{overlap}$ and $T_{step}$, representing the time-horizon from the start of the interval until the next interval. Figure 2.3 clarifies the coherence between the mentioned terms.

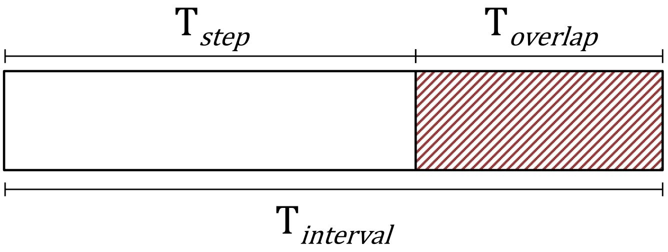

Figure 2.3.: Illustration of the used terms for rolling-horizon time-intervals

To get a better understanding of the fundamental principle of the RH approach, a simple example is given in figure 2.4. It represents an optimization problem with a total problem size of $T$ divided into 4 intervals ($i1...i4$).

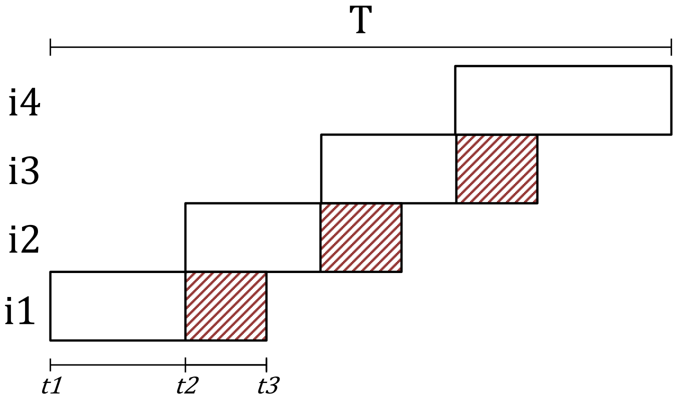

Figure 2.4.: Schematic representation of the rolling-horizon approach

As a first step, interval $i1$ with the interval length of $T_{interval}$ ($t1$ to $t3$) is calculated. The result of $t1$ to $t2$ ($T_{step}$) is later used as a part of the solution while the result of $T_{overlap}$ ($t2$ to $t3$) is not considered anymore. The resulting variables at $t2$ (e.g., the storage level of a seasonal storage) are subsequently passed to the next interval $i2$ and used as start values. The described procedure is then repeated for all intervals and the solution of the total problem $T$ is given by the combination of the results of all time periods $T_{step}$.

Figure 2.4 shows the following coherence:

$$T = I * T_{step} + T_{overlap}, \tag{2.2}$$

with the terms used in figure 2.3, the calculation of the length of a rolling horizon time interval ($T_{interval}$) can generally be formulated as:

$$T_{interval} = \frac{T - T_{overlap}}{I} + T_{overlap} \tag{2.3}$$

Using this calculation of $T_{interval}$, the last interval includes $T_{overlap}$. Another approach would be to let the last interval overlap into the following year.

# 3. Methodology

## 3.1. Handling time-integral constraints

A big weakness of the rolling-horizon (RH) approach is that time-integral constraints, i.e., equations containing variables for each $t \epsilon T$, cannot be modeled in an adequate way. Unlike to a model with perfect foresight, the time horizon used to calculate an interval does not cover the whole time horizon and therefore decision variables can't use the entire information of the model. The following example illustrates that issue using the storage level constraint of long-term storage as a typical example. A simplified equation to calculate the storage level is:

$$S(\tau, y, t) = \sum_{t=1}^{t} P_{in}(\tau, y, t) - P_{out}(\tau, y, t) - P_{loss}(\tau, y, t) \tag{3.1}$$

$$\begin{gathered} \forall\, \tau \,\epsilon\, TEC \\ \forall\, y \,\epsilon\, Y \\ \forall\, t \,\epsilon\, T \end{gathered}$$

With $S(\tau, y, t)$ representing the storage level of a specific storage technology at time $t$. The storage level is calculated by adding inflow and subtracting outflow and losses to the preceding storage level. It is obvious that the equation connects every single time step of $T$. Hence, the optimal dispatch of the storage can only be achieved if the optimization problem is solved considering the full time horizon $T$. Using rolling time horizons, and therefore defining equation 2.1 over $T_{step}$ instead of $T$, the optimal dispatch of the storage cannot be achieved. Instead, the storage will always empty itself towards the end of $T_{step}$. The next figure illustrates that issue looking at the storage level in the first interval $i1$ of a RH example. The storage levels inside $i1$ are represented by the solid lines, the storage levels in interval $i2/T_{overlap}$ are represented by the dotted lines.

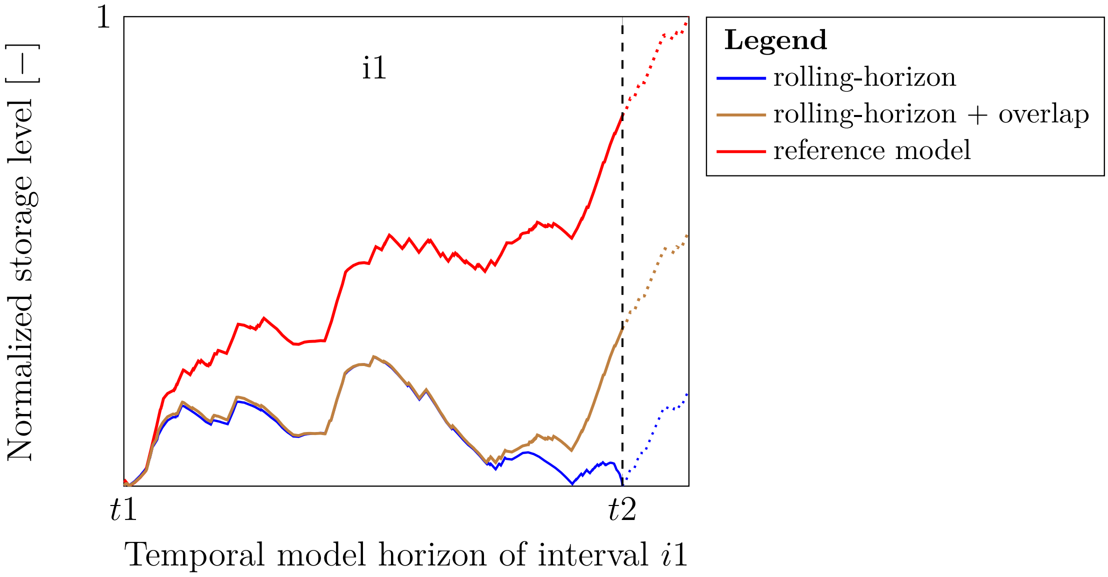

Figure 3.1.: Example demonstrating the usage of overlaps

As expected, if the RH approach is used without providing an overlap (blue line), the storage empties itself towards $t2$. Comparing that behavior with the reference model (red line), i.e., a model solved over the whole time horizon, fundamental differences between the storage levels can be observed. A partly solution of that problem is to use overlaps as described in chapter 2.3. The brown line therefore shows the storage level using RH with an overlap of 80% of the interval size. It can be observed that the storage behavior slightly approximates to the reference model.The big disadvantage of using overlapping time periods is that the problem size, which is tried to be decreased with the RH approach, has to be increased by calculating more time steps. If and how overlaps have an influence on the optimal solution, as well as computational time, will be addressed in chapter 4.

Other time-integral constraints appearing in energy system models are yearly potential limits. A typical example is the yearly $CO_2$ cap. The sum over all $CO_2$ pollutions emitted by all conventional power-plants has to be lower than a certain capacity. Regarding the RH approach, the question of distributing and assigning the $CO_2$ pollution to the single time-intervals arises. One option is to distribute evenly, whereby a mistake is made since the same share of possible $CO_2$ pollution is allocated to intervals with different renewable energy potentials. Other approaches to tackle the problem are explained in chapter 3.2 and 3.4.

## 3.2. Development of a test model

The energy system model REMix consists of a highly complex structure with lots of different sets, variables and equations. An implementation of the rolling-horizon approach therefore takes a lot of effort making model adaptions and testing the model. Hence, it is useful to generate a test model with the main characteristics of REMix.

The test model presented in this section serves two purposes. First, it helps to identify necessary model adaptions to implement a RH approach (e.g. which equations have to be modified). Second, such test environment enables to set up a a hypotheses to answer research questions 2 and 3 (see chapter 1.2).

Features of the test model are:

- Electrical transmission grid of 12 different regions represented through the model nodes $n$
- Yearly time series of electrical load and renewable energy (wind and photovoltaic) input at every node
- 2 different fossil-fired power-plant technologies with different operational costs and emission outputs
- Storage systems with various converter and storage unit capacities at every node

The following figure shows the structure of the test model.

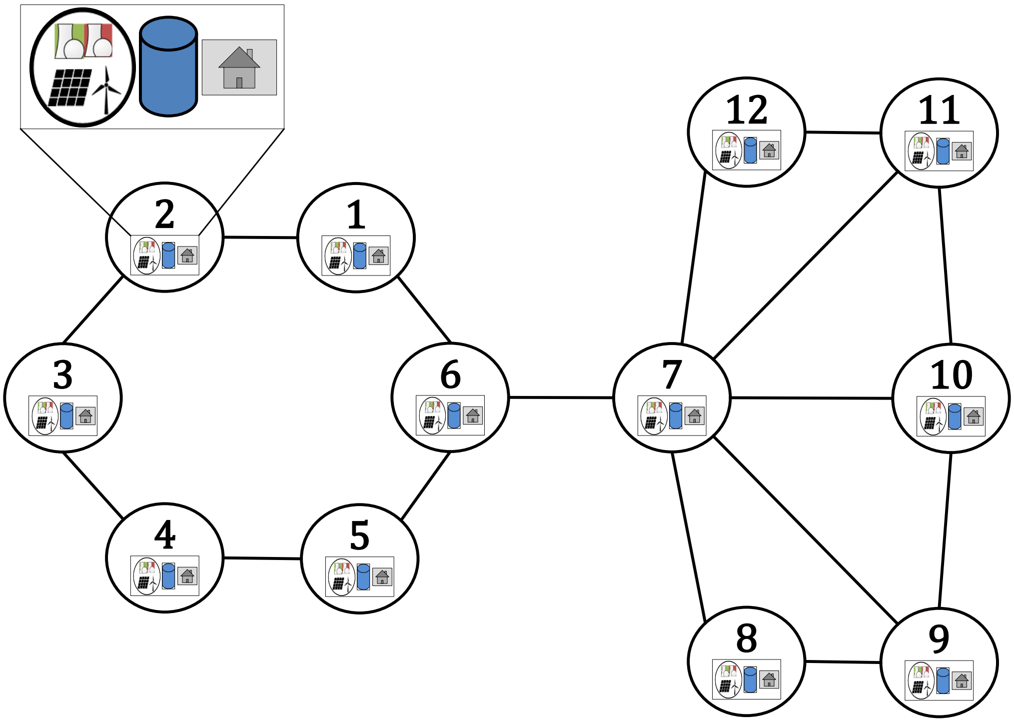

Figure 3.2.: Structure of the simple test model

Two different kinds of grid topologies are represented by the nodes 1-6 (ring network) and 7-12 (mesh network). To enable an energy exchange between the network, different renewable energy potentials, power-plant capacities and storage capacities are assigned to the nodes. In addition, the link between node 6 and 7 ensures an energy exchange between the networks.

The objective function, as well as the most important equations regarding the rolling-horizon approach are illustrated subsequently. Relevant model adaptions deriving from those equations are described. As the test model does not take into account capacity expansion, the objective function only consists of operational costs of the power-plants(pp) (compare chapter 2.1):

$$\sum_{t,\tau,n} c_{pp}(t,\tau,n) \rightarrow min, \tag{3.2}$$

where $c_{pp}$ is a variable associated with the operational costs for each time step $t$, technology $\tau$ and model node $n$. Besides the storage equation (2.1) which can be partially handled by overlaps (compare 2.3), an emission constraint is formulated as:

$$\sum_{t,\tau,n} P_{pp}(t,\tau,n) * e(\tau) \leq E_{max}, \tag{3.3}$$

where $E_{max}$ defines an upper threshold for electricity related emissions (cap) which may not to be exceeded in time horizon $T$. The variable $P_{pp}$ represents the power output of a power-plant and $e_\tau$ the assigned specific emission of the power-plant technology $\tau$.

The simplest way to adjust the equation for the RH approach (distribute the emission cap evenly) was described in section 3.1. This approach can be formulated by changing the equation to:

$$\sum_{\tau,n} \sum_{t=t_1(i)}^{t_2(i)} P_{pp}(t,\tau,n) * e(\tau) \leq \frac{T_{step}}{T} * E_{max} \tag{3.4}$$

Whereby this equation applies for each interval $i$ of the time horizon $T$. The indices of $t$ ($t_1$, $t_2$) represent the start and end points of the respective time horizon $T_{step}$ (compare chapter 2.3). If $t_3$, i.e. the end point of the whole time interval including the $T_{overlap}$, would be used as an upper bound of the sum, the result could be infeasible. This is due to the global constraint on the emission (equation 3.3). Using $t_3$ instead of $t_2$ and $T_{overlap}$ in place of $T_{step}$, the power-plants could generate too much emission in the period $T_{step}$ and therefore the global emission (sum over all interval emissions) could be higher than $E_{max}$.

Another approach to handle equation 3.3 is described in the following section. Similar to REMix, the renewable energy potential and electrical load are exogenous model parameters in the test model. The needed conventional power-plant output and linked emissions in each interval depend on the renewable energy production and load in this interval. Hence, the residual load $P_{res}(t)$ (total load - renewable energy production) can be used as a parameter to distribute the emission cap to the time intervals. The resulting equations can be written as:

$$\sum_{\tau,n} \sum_{t=t_1(i)}^{t_2(i)} P_{pp}(t,\tau,n) * e(\tau) \leq \frac{\sum_{t=t_1(i)}^{t_2(i)} P_{res}(t)}{\sum_t^T P_{res}(t)} * E_{max}, \quad \forall\, i \,\epsilon\, I \tag{3.5}$$

This equation assures that each time interval $i$ receives an emission cap dependent on the relative residual load. That means that an interval with low residual load, i.e., a high penetration of renewable energies, is assigned with a small emission cap and an interval with a high residual load with a bigger emission cap.

## 3.3. Implementation in REMix

### 3.3.1. Definition of a reference model

A reference model has to be set up as a basis for the evaluation of the RH approach. This reference model has to meet several requirements. It has to be solvable in a reasonable time, because a parameter study will be performed varying the number of intervals and overlap sizes. To analyze the effects of time-integral constraints (as described in chapter 3.1), technologies like storage systems and biomass power-plants have to be included in the model. Also, the model should be based on a scenario including capacity expansion. In this way expansion planning can be provided endogenously by the model to use it as a foundation for a dispatch model (see chapter 4.2). Yet it can also be used to evaluate expansion planning and dispatch using the temporal-hierarchical approach presented in chapter 3.4.

The following table shows the basic configuration of the used model which meets the described requirements:

Table 3.1.: Profile of the reference model

| | |
|---|---|
| **Model name** | REMix |
| **Model type** | Least-cost system configuration and operation |
| **Geographical focus** | Germany |
| **Technical focus** | Coverage of the electrical demand |
| **Spatial Resolution** | 20 regions based on [10] |
| **Temporal resolution** | 1h steps |
| **Temporal Horizon ($T$)** | 8760h |
| **Considered technologies** | Conventional power-plants<br>Wind, solar and run-of-river power-plants<br>Biomass power-plants<br>Pumped-storage power-plants |

Input parameters and their temporal, technological and spatial dependencies are listed in the next table. The input parameters listed below are based on [11] representing data of the scenario year 2050.

Table 3.2.: Input parameters of the reference model and their dependencies

| **Input parameter** | **Dependencies** | | |
|---|---|---|---|
| | Temporal | Technological | Spatial |
| Efficiencies | | x | |
| Potential limits and technical restrictions | | x | |
| Operational costs | | x | |
| Investment costs | | x | |
| Fuel costs and certificate costs | | x | |
| Electrical demand and renewable energy profiles | x | | x |

The output of the model is on the one hand, the optimal dispatch of the generation power-plants. On the other hand, if capacity expansion is not predefined, the cost-optimal expansion of the technologies listed in table 3.1. The presented reference model matches the earlier defined requirement, since the spatial resolution was chosen in a way that results in reasonable computing times. Besides, technologies like biomass power-plants and pumped-storage power-plants are modeled with time-integral constraints. Furthermore, the conventional power-plants are restricted by emission constraints which also represent time-integral constraints.

### 3.3.2. Adjustment of the solve statement

After illustrating the required adjustments of time-integral equations (see 3.1 and 3.2) further essential model adjustments are presented now. In the case of a RH approach, it is obvious that the optimization model is not solved using the overall time horizon $T$. In a first step $T_{interval}$ needs to be generated for every RH interval. This is achieved by employing equation 2.3 with $I$ and $T_{overlap}$ as input parameters. With the information of the time model of each interval $i$, the solve statement can be formulated as a loop, calculating the intervals iteratively. The following flow chart demonstrates the adjusted solve statement:

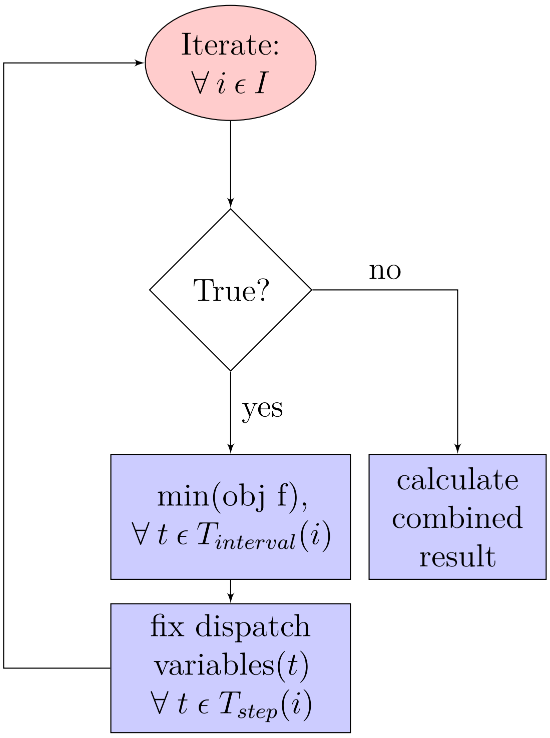

Figure 3.3.: Rolling-horizon loop flow chart

The main component is a loop over all intervals $I$. As a first step in the loop, the model is solved minimizing the objective function (see 2.1) for the current time interval $T_{interval}$. Afterwards, the results for all decision variables depending on $t$ are fixed over the time horizon $T_{step}$. It has to be emphasized that the variables are only fixed for $T_{step}$, since the variables for $T_{overlap}$ are not used anymore after the iteration. After the last iteration, the combined result of all intervals is calculated. This is performed by simply using the fixed variables of the whole time horizon $T$ and calculating the objective value. It is important to perform the last calculation of the combined result to check if the global constraints are not violated.

## 3.4. Temporal-hierarchical approach to improve rolling-horizon

As described in chapter 3.1, the RH approach is not suited to model time-integral constraints such as seasonal storage or emission limits. Also, capacity expansion was not considered until now. A common approach (compare [12]) is to solve the linear problem with a lower time resolution than $1h$ (e.g.,$12h$, $24h$, $48h$,...) in advance of the RH approach, important information can be provided. Figure 3.4 outlines the principle of this "temporal-hierarchical approach":

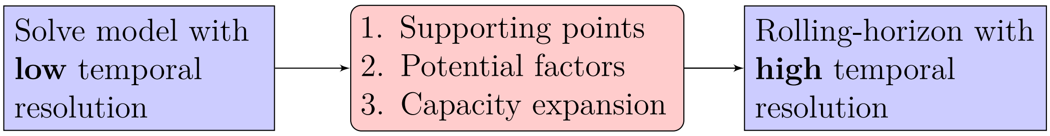

Figure 3.4.: Functional principle of the temporal-hierarchical approach

First, the model is solved over the time horizon $T$ with a low temporal resolution. Information about sampling points, potential factors and capacity expansions are then passed to the RH approach which solves the model iteratively with a high resolution. Why and how the passed information (red block) is used, will be described as follows.

### 1. Supporting points

Supporting points are needed to address the problem of seasonal storage described in 3.1. For every start and end point of a time interval $i$ the values for the storage level are fixed, employing the result of the model solved with low temporal resolution. Therefore, the behavior of the the seasonal storage approximates to the global solution with a high ($1h$) temporal resolution. The principle of supporting points is illustrated for a small example in figure 3.5. The diagram shows the normalized storage level (y-axis) of a seasonal storage. For each, a low resolution result, a high resolution result and the result of a RH approach with 4 intervals is depicted. The time horizon $T$ (x-axis) is divided into 4 intervals ($i1..i4$).

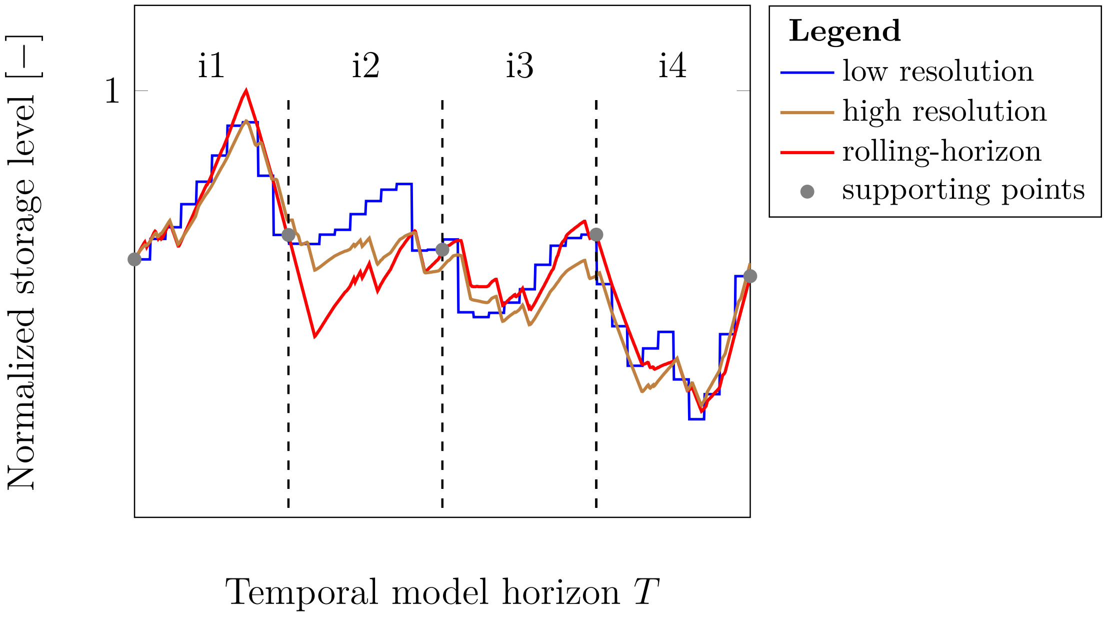

Figure 3.5.: Principle of supporting points to model seasonal storage

The blue graph, representing the model output of a model with low temporal resolution, shows the behavior of a step-function.

This is because the model uses average values dependent on the temporal resolution. The diagram shows that the intersection between the blue graph and the start and end values of every interval $i$ are used as supporting points (gray dots). It can be observed that the result of the RH approach (red line) approximates to the low resolution run using the supporting points. More importantly, it also approximates the high resolution dispatch behavior between the sampling points (brown line).

### 2. Potential factors

Besides the issue of modeling seasonal storage with a RH approach, the problem of global potential restrictions (see chapter 3.1) has to be solved in an adequate way. For that reason, potential factors are introduced. With the use of the low resolution result, these potential factors are calculated for each interval with the goal of distributing the total potential to the intervals. For the example described in equation 3.3, the potential factors are calculated as:

$$\rho(i) = \frac{\sum_{t=t_1(i)}^{t_2(i)} P_{pp}(t, \tau, n) * e(\tau)}{\sum_{t=t_1}^{T} P_{pp}(t, \tau, n) * e(\tau)} \tag{3.6}$$

$$\forall\, t \,\epsilon\, T_{lowres}$$
$$\forall\, i \,\epsilon\, I$$

Inserted in equation 3.7, substituting $\frac{T}{T_{step}}$, one receives:

$$\sum_{\tau,n} \sum_{t=t_1(i)}^{t_2(i)} P_{pp}(t, \tau, n) * e(\tau) \leq \rho(i) * E_{max} \tag{3.7}$$

The described potential factors can also be used for other potential limit constraints like a limit on yearly biomass for biomass power-plants.

### 3. Capacity expansion

As mentioned previously, the RH approach is not suitable for capacity expansion planning. That is because the full time horizon of a model has to be known to perform optimal investment decisions. Here again, the temporal-hierarchical approach can provide a rough solution. The expansion of capacity (e.g., power-plants, transmission lines,..) can be used and set as a lower bound for the RH approach. As a result, additional investments needed to cover peak loads can be performed in the respective time intervals of the RH approach.

## 3.5. Identifying relevant indicators for the evaluation

The results of the RH parameter study in chapter 4 are compared to the results of the reference model with a high temporal resolution. In order to compare the quality of the RH results with the reference model, relevant indicators are needed. The following table gives an overview on the used indicators and the assertions they make or questions they try to answer.

Table 3.3.: Indicators to analyze and compare the rolling-horizon with the reference case

| **Analysis** | **Indicator** |
|---|---|
| Can a significant reduction in computational time be achieved? | Computation time |
| First impression of the similarity of both results | Objective value |
| How big is the deviation in the operation of technologies affected by time-integral constraints? | Total yearly $CO_2$ emissions |
| Is the rolling-horizon approach capable of modeling seasonal storage? | Temporal profile of seasonal storage |

Since the objective value only represents the investment and operational costs, indicators like the total $CO_2$ emissions are chosen to compare the RH result with the "global" result. The presented indicators will also be used to compare the rolling-horizon approach with the advanced temporal-hierarchical approach.

# 4. Results and analysis

### Simulation environment

The subsequently presented results are all computed in the same simulation environment. Hardware settings of the machine are:

- Intel Xeon CPU X5650 @2.67 GHz with 6 cores
- 96 Gb of Ram

IBM ILOG CPLEX ([13]) is used to solve the model generated by GAMS ([6]). CPLEX is set up using 1 thread and the barrier optimizer, which uses the interior point method ([14]) as a solving algorithm. In the further course of the work, the required time to generate the model along with the translation of the model to a CPLEX readable code is referred to as model-generation-time. The time needed by the algorithm to solve the linear problem is referred to as CPLEX-time and the combination of both, i.e. the total computation time, is denoted as computational-time.

## 4.1. Evaluation of the test model

### CPLEX-time

One of the objectives of the test model is to estimate the possible reduction of computational-time in REMix through the application of the RH approach. As the test model does not use the exact same modeling approach as REMix, only the CPLEX-time is evaluated in the following parameter study of the test model. The table below shows the CPLEX-time for RH runs with varying interval-sizes (column entries) and step-sizes (row entries). Fast values of CPLEX-time are marked in green and slow values in red respectively. $T_{interval}$ and $T_{step}$ are presented as hours (h) as well as days (d), weeks(w) and months(m). As explained in chapter 2.3, $T_{interval} - T_{step}$ describes $T_{overlap}$. Therefore, diagonal entries of the table represent a model without overlaps. Starting from a diagonal entry, the overlap-size increases from the bottom to the top. Reading the table from left to right for a specific row, the overlap-size also increases as $T_{step}$ is fixed and $T_{interval}$ increases.

Table 4.1.: CPLEX-time [s] for different interval and step sizes

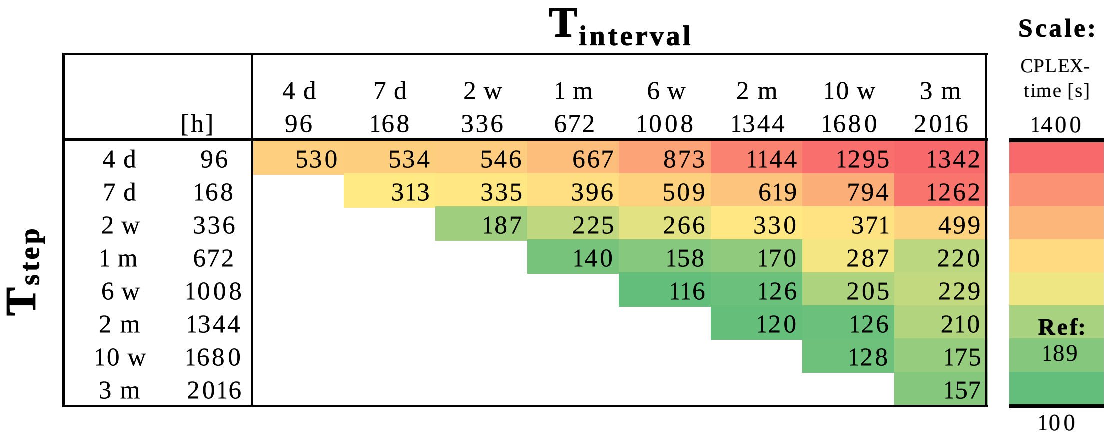

| | [h] | 4 d<br>96 | 7 d<br>168 | 2 w<br>336 | 1 m<br>672 | 6 w<br>1008 | 2 m<br>1344 | 10 w<br>1680 | 3 m<br>2016 |
|---|---|---|---|---|---|---|---|---|---|
| 4 d | 96 | 530 | 534 | 546 | 667 | 873 | 1144 | 1295 | 1342 |
| 7 d | 168 | | 313 | 335 | 396 | 509 | 619 | 794 | 1262 |
| 2 w | 336 | | | 187 | 225 | 266 | 330 | 371 | 499 |
| 1 m | 672 | | | | 140 | 158 | 170 | 287 | 220 |
| 6 w | 1008 | | | | | 116 | 126 | 205 | 229 |
| 2 m | 1344 | | | | | | 120 | 126 | 210 |
| 10 w | 1680 | | | | | | | 128 | 175 |
| 3 m | 2016 | | | | | | | | 157 |

Compared to the reference case (CPLEX-time of 189s), a reduction of the computational time can only be achieved using $T_{step}$ in a range of 672h-2016h, i.e. 5-13 intervals, without or only with a slight overlap (dark green entries). Ranging from 116s-170s, these set ups of $T_{step}$ and $T_{interval}$ reduce the computational time by 10-39%. Using small step sizes and big interval sizes, i.e. a big $T_{overlap}$, the computational times are multiple times higher than the reference case (dark red area).

The observed results indicate two main circumstances. First, it can be observed that with the same $T_{interval}$, the CPLEX-time increase along with a decreasing $T_{step}$. This can be contributed to the increasing problem size related to an increasing $T_{overlap}$. Second, only considering diagonal entries of the table, an optimum in the reduction of CPLEX-time can be achieved with a $T_{step}/T_{interval}$ of about 1008h which translates into a RH setting of 9 intervals.

### Objective Value

Besides the primary objective of reducing the computational time, the RH approach should also deliver a result similar to the reference case. A first indicator for the similarity is the objective value, which is calculated using equation 3.2. The following table shows the percentage deviation of the objective value for varying $T_{step}$ and $T_{interval}$. The table can be read the same way as described for the previous table.

Table 4.2.: Deviation of the objective value to the reference case [%]

$T_{interval}$

| $T_{step}$ | [h] | 4 d<br>96 | 7 d<br>168 | 2 w<br>336 | 1 m<br>672 | 6 w<br>1008 | 2 m<br>1344 | 10 w<br>1680 | 3 m<br>2016 |
|---|---|---|---|---|---|---|---|---|---|
| 4 d | 96 | 0.47 | 0.49 | 0.40 | 0.33 | 0.31 | 0.31 | 0.28 | 0.25 |
| 7 d | 168 | | 0.35 | 0.20 | 0.23 | 0.22 | 0.21 | 0.19 | 0.17 |
| 2 w | 336 | | | 0.11 | 0.17 | 0.16 | 0.15 | 0.14 | 0.12 |
| 1 m | 672 | | | | 0.09 | 0.12 | 0.12 | 0.12 | 0.12 |
| 6 w | 1008 | | | | | 0.14 | 0.12 | 0.12 | 0.09 |
| 2 m | 1344 | | | | | | 0.10 | 0.10 | 0.10 |
| 10 w | 1680 | | | | | | | 0.13 | 0.11 |
| 3 m | 2016 | | | | | | | | 0.11 |

**Scale:**

Deviation obj. Value [%]

0.5

0.1

Table 4.2 shows that the deviation of the objective value is within a range of 0.09% to 0.47% for all RH instances. The best results, i.e. the smallest deviation, is achieved using a big $T_{step}$ (green data at bottom right). Another effect which can be observed is the tendency of an increasing deviation with decreasing $T_{step}$ (increasing $T_{overlap}$ respectively).

Overall, the presented results show a negligible deviation of the objective value. This can be explained through the objective function (equation 3.2) which takes into account the operational costs of the conventional power-plants. As the emission cap for the mentioned is distributed to the intervals using equation 3.7, the dispatch of the conventional power-plants does not have an essential influence on the objective value. The table also shows the tendency of an increasing deviation along with a decreasing $T_{step}$. This however suggest that an increasing overlap causes none or a negative influence on the objective value, although an increasing overlap aims to improve the behavior of model components like seasonal storage. This is due to the assumed modeling parameters of the storage in the test model. The storage in the test model are modeled as short-term storage. Hence, their charge and discharge cycles take place in short time periods, e.g. several hours or days. The expected positive effect on seasonal-storage therefore cannot be observed in the table.

## 4.2. Rolling-Horizon dispatch in REMix

In this section, the implementation of the RH dispatch is evaluated using a parameter study. Therefore the analysis of the indicators presented in chapter 3.5 is performed for varying numbers of intervals (2,4,6,8,10,20,30,40,50,60,70,80,100) and relative overlap-sizes (0%,20%,40%,60%,80%,100%,200%), to figure out the most effective settings of the RH approach for the evaluated reference model. Only selected results of the parameter study are evaluated in the following section. The full results of each evaluation are shown in the appendix (see section A.1).

### 4.2.1. Reduction of the computational-time

This section analyzes the dependency of the computational-time to the number of intervals and overlap-sizes. As the main aim of the RH approach is a reduction of computational-time, this evaluation helps to filter out relevant parameters for the further analysis. The following scatter plot shows the relative deviation of the computational-time to the reference model for different overlap-sizes over the number of intervals.

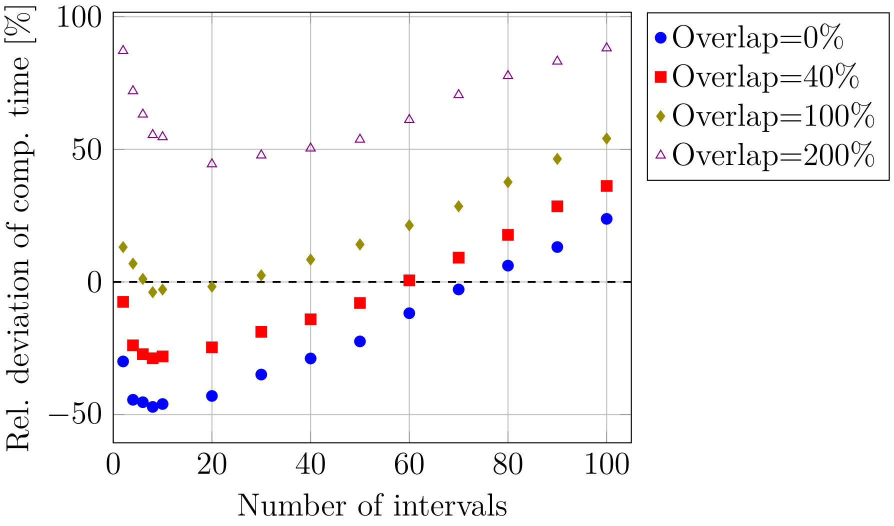

Figure 4.1.: Computational time for different rolling-horizon settings as a relative deviation from the reference model

A first glance at the figure shows a similar trend of the data independent of the overlap-size. Starting from 0 to 100 intervals, an initial decrease of the y-value followed by an increase can be observed. As the y-axis represents the relative deviation of computational time to the test model, values above 0 represent an increase of computational-time whereas values below 0 represent a decrease of computational-time. Hence, the figure shows that using an overlap-size of 200% leads to an increase in computational time independent of the number of intervals. Likewise, an overlap of 100% leads to an increase of computational time for almost any number of intervals. A decrease is only being achieved for small or no overlap-sizes with a number of intervals ranging from 2-70. The highest decrease in computational time (the minima of the scatter plots) of about -50% is achieved using 8 intervals and no overlaps. For the same amount of intervals and an overlap-size of 40% a reduction 30% is achieved.

The observed data confirms the results of the test-model, since it shows that big overlaps as well as a big number of intervals lead to an increase of computational-time. Furthermore, the best result is achieved with a similar amount of 8 intervals (9 intervals in the test model). As all data points and their related parameters above the x-axis fail the aim of a reduction of computational-time, they will not be considered in the further evaluation of the results. The shape of the scatter plots can be attributed to two effects. First, the effect of increasing computational-time occuring with an increasing number of intervals after reaching a minimum value, is due to an increasing model-generation-time with a growing number of intervals. As a hypothesis, the positions of the minima can be explained by scaling effects of the solver algorithm. Until a certain point, a decrease of the problem size, i.e. more intervals, leads to savings in computation time. After that point (observed minima in figure 4.1) is reached , the decrease of computational time does not further scale for an increasing amount of intervals.

### 4.2.2. Deviation of the objective value

The objective value analyzed in this section represents the total operational costs of all power-plants (compare equation 2.1). Therefore, the objective value of the reference model provides the information about the optimal dispatch of all power-plants and storage units within the whole time-horizon $T$. In order to get a first indication of the quality of the RH result, a comparison to the objective value gives a rough assessment of the similarity of both dispatch behaviors. Table 4.3 provides the relative deviation of the objective value of the RH model to the reference model. Not all parameter values of the parameter study are shown as some of them are not suitable due to an increase of computational-time (as described in section 4.2.1).

Table 4.3.: Relative deviation of the rolling-horizon objective value to the reference model for varying number of intervals and overlap-sizes

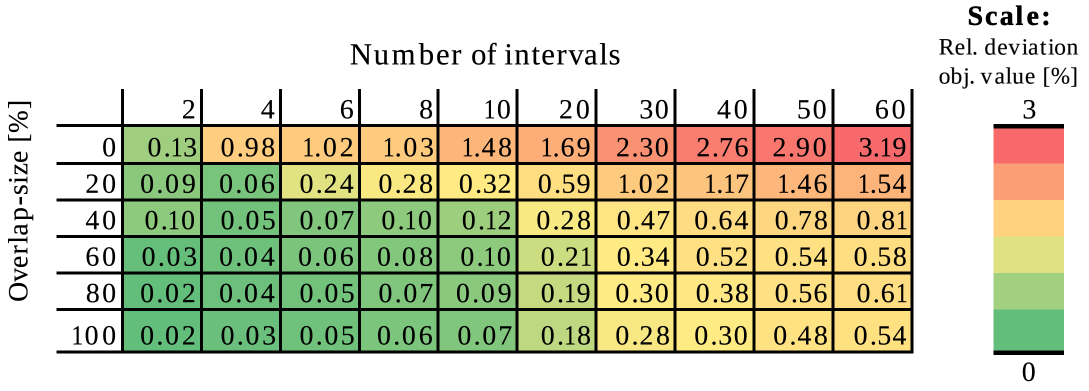

Number of intervals

| Overlap-size [%] | 2 | 4 | 6 | 8 | 10 | 20 | 30 | 40 | 50 | 60 |
|---|---|---|---|---|---|---|---|---|---|---|
| 0 | 0.13 | 0.98 | 1.02 | 1.03 | 1.48 | 1.69 | 2.30 | 2.76 | 2.90 | 3.19 |
| 20 | 0.09 | 0.06 | 0.24 | 0.28 | 0.32 | 0.59 | 1.02 | 1.17 | 1.46 | 1.54 |
| 40 | 0.10 | 0.05 | 0.07 | 0.10 | 0.12 | 0.28 | 0.47 | 0.64 | 0.78 | 0.81 |
| 60 | 0.03 | 0.04 | 0.06 | 0.08 | 0.10 | 0.21 | 0.34 | 0.52 | 0.54 | 0.58 |
| 80 | 0.02 | 0.04 | 0.05 | 0.07 | 0.09 | 0.19 | 0.30 | 0.38 | 0.56 | 0.61 |
| 100 | 0.02 | 0.03 | 0.05 | 0.06 | 0.07 | 0.18 | 0.28 | 0.30 | 0.48 | 0.54 |

The presented table shows two distinct trends. First, reading the table from left to right, an increase of the number of intervals goes along with an increasing deviation to the reference case. Second, reading the table top down, an increase of the overlap-size achieves an improvement of the accuracy of the objective value. Hence, the relative deviation ranges from 0.02% (best case, bottom left) to 3.19 % (worst case, top right).

Unlike the results provided by the test model, Table 4.3 shows that the overlap-size decreases the relative deviation of the objective value. Moreover, it shows that a high number of intervals, i.e. a small $T_{interval}$, leads to an inaccurate model result. The observed effects suggest that the dispatch behavior of power-plants and seasonal-storage units improve with an increasing model horizon due to the greater consideration of time-integral constraints (compare chapter 3.1). In order to find out in which exact way time-integral constraints effect the model results, the subsequent sections deal with indicators affected by time-integral constraints.

### 4.2.3. Effects of time-integral constraints

After analyzing the issue of time-integral constraints and suggesting the use of overlaps as a partial solution in chapter 3.1, this section quantifies the effect of the different overlap-sizes and numbers of intervals on the constrained variables.

#### Temporal profile of seasonal storage

As described in chapter 3.1, it is necessary to calculate the storage level of a storage (equation 2.1) over a sufficiently sized $T_{interval}$ to receive an approximate solution to the reference model. In order to quantify the influence of overlap-sizes and number of intervals on the temporal profile of the storage, the person correlation coefficient (PCC) is used as a measurement of linear correlation between the temporal storage profiles of the RH result and the reference model. In general, the PCC for two data-sets $(X(x_1, ..., x_n),(Y(y_1, ..., y_n))$ with $n$ values is calculated as:

$$r(X,Y) = \frac{cov(X,Y)}{\sigma_X * \sigma_Y} = \frac{\sum_{i=1}^{n}(x_i - \bar{x})(y_i - \bar{y})}{\sqrt{\sum_{i=1}^{n}(x_i - \bar{x})^2(y_i - \bar{y})^2}}, \tag{4.1}$$

with $cov(X,Y)$ as the covariance of $X, Y$, $\sigma$ as the standard deviation and $\bar{x}$, $\bar{y}$ as the mean of the sample value.

In order to compare the temporal profiles (reference model $ref$ and rolling-horizon model $rh$) of a specific seasonal storage $\alpha$, the above equation can be reformulated as:

$$r_\alpha(ref,rh) = \frac{\sum_{t=1}^{T}(S_{\alpha,ref}(t) - \bar{S}_{\alpha,ref}(t))(S_{\alpha,rh}(t) - \bar{S}_{\alpha,rh}(t))}{\sqrt{\sum_{t=1}^{T}(S_{\alpha,ref}(t) - \bar{S}_{\alpha,ref}(t))^2(S_{\alpha,rh}(t) - \bar{S}_{\alpha,rh}(t))^2}}, \tag{4.2}$$

where $S_{\alpha,t}$ represents the storage level of a seasonal storage at time-step $t$. The PCC ($r$) can obtain values between -1 and 1. Using the example of equation 4.2, the interpretation of the value range of $r$ can be formulated as:

- $r > 0$ represents a positive correlation, i.e. the values of the storage levels tend to increase and decrease simultaneously
- $r < 0$ represents a negative correlation, i.e. the values of the storage levels tend to increase and decrease in the opposite direction
- $r = 0$ represents no correlation, i.e. the values of the storage levels neither increase nor decrease together in a certain pattern

The application of the PCC on the results of the RH parameter study is illustrated using the figure below. In order to examine the influence of the overlap-size on the temporal storage profile, the figure shows the normalized storage level over the time-horizon $T$ for two RH settings using the same number of intervals (8) and different overlap-sizes (0% and 200%). These results are compared to reference model.

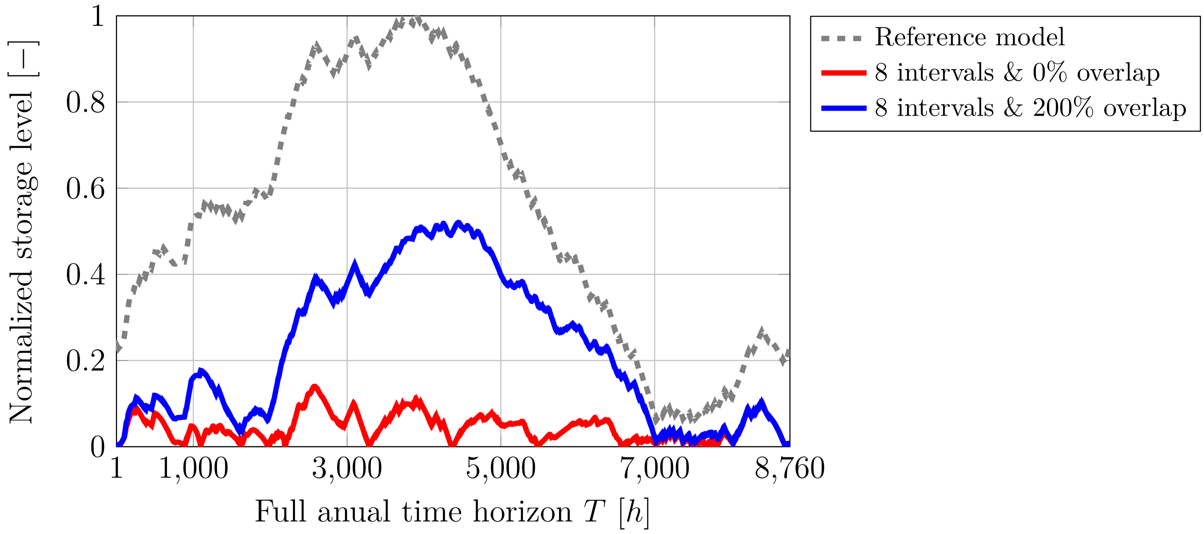

Figure 4.2.: Normalized storage level over $T$ for different modeling approaches

As described in chapter 3.1 the use of overlaps improves the result as the profile of the storage (blue line) approximates to the reference model in its behavior. A y-axis offset between the RH curves and the reference model can be observed. This offset can be ascribed to the formulation of the storage equation in the reference model, which constrains the start and end value of the storage level to be identical, independent of their value. Regardless of the y-axis offset of the reference model, the storage levels seem to be similar in their profiles. This results in a $r_\alpha$ of 0.84 using an overlap-size of 200% (blue line). In contrast, the temporal profile of the RH result with no overlap (red line) shows the behavior described in chapter 3.1. Towards each end of a time period, the storage empties itself. Hence, the global course of the graph is not comparable to the reference model. Still, between the start and end points of the intervals a similar behavior in comparison to the reference model can be observed (for example the two significant peaks between 2000h and 4000h). Both mentioned aspects of the observed behavior result in a $r_\alpha$ of 0.56.

The example described above only refers to a single storage unit $\alpha$ of the whole model. For further analysis, the mean value of all PCCs ($\bar{r}$) over all seasonal storage in the model is used:

$$\bar{r} = \frac{\sum_{\alpha=1}^{A} r_\alpha}{A}, \tag{4.3}$$

where $A$ represents the number of all storage units in the model. Table 4.4 shows $\bar{r}$

for the same parameters of overlap-size and number of intervals as presented in section 4.2.2.

Table 4.4.: Mean correlation coefficient $\bar{r}$ for a different number of intervals and varying overlap-sizes

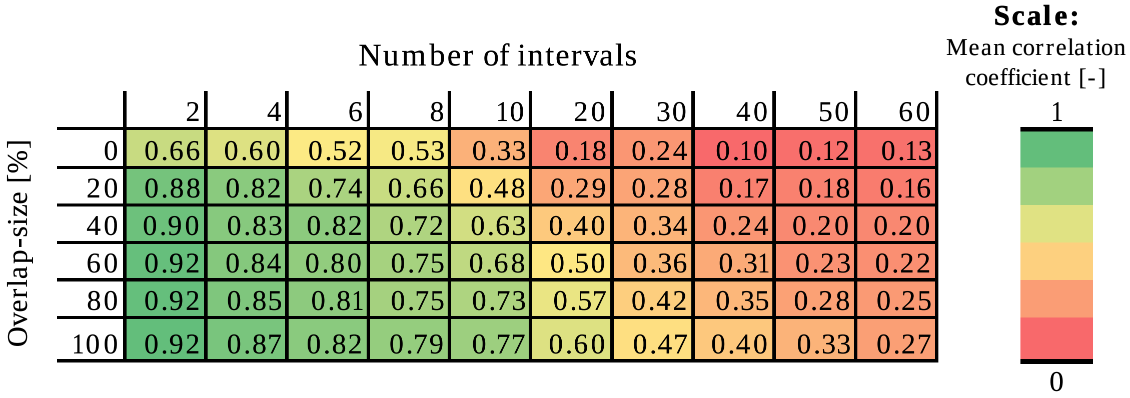

| Overlap-size [%] | Number of intervals | | | | | | | | | |
|---|---|---|---|---|---|---|---|---|---|---|
| | 2 | 4 | 6 | 8 | 10 | 20 | 30 | 40 | 50 | 60 |
| 0 | 0.66 | 0.60 | 0.52 | 0.53 | 0.33 | 0.18 | 0.24 | 0.10 | 0.12 | 0.13 |
| 20 | 0.88 | 0.82 | 0.74 | 0.66 | 0.48 | 0.29 | 0.28 | 0.17 | 0.18 | 0.16 |
| 40 | 0.90 | 0.83 | 0.82 | 0.72 | 0.63 | 0.40 | 0.34 | 0.24 | 0.20 | 0.20 |
| 60 | 0.92 | 0.84 | 0.80 | 0.75 | 0.68 | 0.50 | 0.36 | 0.31 | 0.23 | 0.22 |
| 80 | 0.92 | 0.85 | 0.81 | 0.75 | 0.73 | 0.57 | 0.42 | 0.35 | 0.28 | 0.25 |
| 100 | 0.92 | 0.87 | 0.82 | 0.79 | 0.77 | 0.60 | 0.47 | 0.40 | 0.33 | 0.27 |

An increase of intervals (horizontal values) trends to reduce the correlation coefficient and an increasing overlap-size (vertical values) increases the correlation coefficient. The overlayed heatmap of the table shows the same pattern as observed in table 4.3 (relative deviation of the objective value) with $\bar{r}$ ranging from 0.1 to 0.92. Hence, it can be concluded that one of the reasons of the observed pattern of the objective value for varying parameters can be attributed to the suboptimal modeling of seasonal storage for an increasing number of intervals.

### Annual carbon emissions

In order to evaluate the power-plant dispatch for the parameter study, the annual carbon emissions are assessed. The parameter of carbon-certificate-costs of the reference model scenario is chosen to be high relative to the operational costs. Since $CO_2$-emissions certificate costs do not affect the dispatch of biomass power-plants due to their $CO_2$ neutrality, the operational costs of the conventional power-plants exceed the operational costs of the biomass power-plants. As the mentioned power-plants represent the total variable generation in the model, a low-cost dispatch manifests in a low usage of conventional power-plants and a high usage of biomass power-plants. High annual carbon emissions therefore represent a high ratio of conventional power-plant production to biomass power-plant production. The following bar chart shows the increase of carbon emission relative to the reference model for a selected number of intervals and 3 different overlap-sizes.

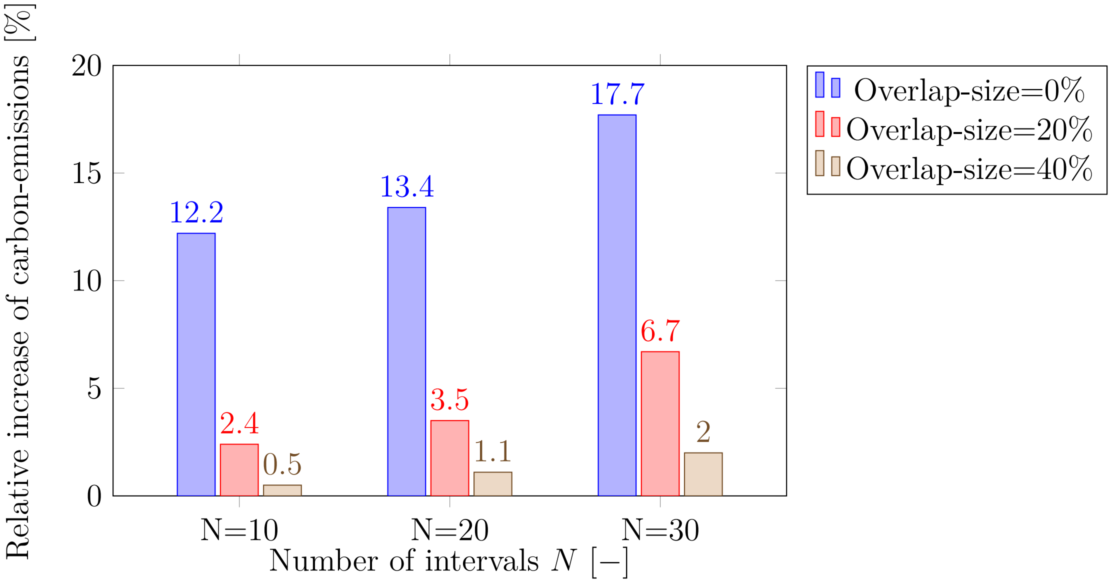

Figure 4.3.: Relative increase of carbon-emissions in relation to the reference model for selected number of intervals and overlap-sizes

The bar chart displays two main parameter relations. First, using an overlap-size of only 20% or 40% regardless of the number of intervals, a much lower increase of relative carbon-emission can be observed. Second, similar to the previous evaluations, a decline of the quality of the result, i.e. relative deviation to the reference model, can be observed with an increasing amount of intervals.

The mentioned effects can be traced back to the time-integral constraint of the biomass production limit. In the reference case the energy production of the biomass power-plant can be distributed optimally over the whole time-horizon $T$. Hence, an optimal dispatch resulting in a minimum of carbon-emission can be achieved, since the energy output of conventional power-plants is minimized and the optimal use of biomass power-plants is ensured. Increasing the number of intervals and therefore decreasing $T_{interval}$ leads to two limitations of the dispatch behavior. First, a decreasing flexibility of operation due to a suboptimal balancing of intermittent renewable energy production. Another important aspect related to the time-integral constraints of the potential limit, is that the same amount of biomass-potential is assigned to each interval relative to $T_{step}$ (compare equation 3.7). Hence, the same biomass-potential can be assigned to an interval with a high need of additional biomass-energy or a low need of additional biomass-energy respectively. A small interval-size therefore leads to a restricted dispatch behavior, which again results in an increase of carbon-emissions.

## 4.3. Rolling-Horizon dispatch using a temporal-hierarchical approach

The results presented in the previous section revealed that, despite the use of overlaps, the RH approach is not suitable to handle time-integral constraints for a big number of intervals. This section evaluates the temporal-hierarchical (TH) approach presented in section 3.4 using a previous low resolution model result as an input for the RH approach. The first subsection focuses on the achieved improvement through the temporal-hierarchical approach especially regarding the results of section 4.2.3. The second subsection deals with the influence of the temporal resolution of the low resolution model on the RH results. Therefore the TH approach is applied using 6h, 12h and 24h as a temporal resolution of the low resolution model.

### 4.3.1. Improvement of the rolling-horizon result

In order to evaluate the improvement achieved through the temporal-hierarchical approach, the results of the "regular" RH with no overlap are compared to the TH approach with a temporal resolution of 12h. The main indicators evaluated in chapter 3.5 are compared for 4, 20 and 40 intervals in the following figures.

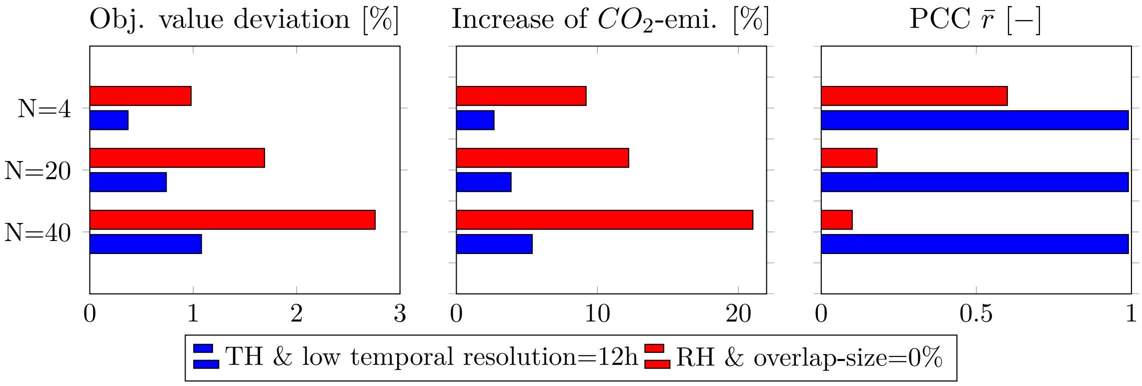

Figure 4.4.: Comparison between the regular RH approach and the TH approach for main indicators

The figure on the left-hand side shows the deviation of the objective value relative to the reference model for each, the regular RH approach and the TH approach. It can be observed that regardless of the number of intervals, the TH approach improves the result significantly. In the worst case ($N = 40$) the relative deviation of the objective is reduced by a factor of 2.6 from 2.76% to 1.08%. For $N = 20$ and $N = 4$ a reduction from 1.69% to 0.74% and 0.98% to 0.37% is achieved.

One of the causes of that reduction can be explained by the middle plot. As demonstrated in chapter 4.2.3, the increase of $CO_2$-emissions indicates a limited, non-optimal scheduled dispatch behavior of the power-plants. The TH approach reduces that effect in a similar way as observed in the left figure. This is due to the improved distribution of potential limits to the intervals using the information of the low resolution result (compare equation 3.6). Hence, a significant absolute reduction of $CO_2$-emissions can be observed especially for a high number of intervals. For 40 intervals, an absolute reduction of 15.6 percentage points (from 21% to 5.4%) is achieved.

The bar chart on the right-hand side compares the mean correlation coefficient ($\bar{r}$) of both approaches. As described in section 3.4 the temporal profile of seasonal storage is improved using supporting points at the start and end of each interval. Similar to the evaluation in the previous chapter, the correlation coefficient is used to assess the storage behavior. The bar chart proves the effect of the supporting points. Regardless of the number of intervals, the value of $\bar{r}$ is approximately 1 for the TH approach, while $\bar{r}$ decreases for increasing number of intervals for the regular RH approach.

## 4.3.2. Influence of the temporal resolution

The previous section only analyzed the effect of the temporal-hierarchical approach for a temporal resolution of the input data of 12h. As the calculation of the low resolution result goes along with an increase of the total computational time, it has to be evaluated which temporal resolution is sufficient to improve the RH approach without increasing the computational time in a non reasonable way. As a first step to assess this issue, the following table shows the possible reduction of computational-time compared to the reference model using the TH approach for temporal resolutions of the low resolution of 6h,12h,24h using 8 intervals.

Table 4.5.: Relative reduction of computational-time for the evaluated temporal resolutions of the TH approach

| **Temporal resolution** [$h$] | 6 | 12 | 24 |
|---|---|---|---|
| **Relative reduction of computational-time** [%] | 35 | 40 | 43 |

Without factoring in the additional time required to calculate the low resolution model, a relative reduction in computational-time of 46% can be achieved. Table 4.5 shows that the use of a resolution of 6h decreases the computational-time by 11 percentage points compared to the possible total reduction of computational-time. For decreasing temporal resolutions, a convergence towards 46% can be observed. In order to evaluate the influence of the temporal resolution on the results, the following figures compare the results of the same indicators as presented in the previous section for varying temporal resolutions (6h,12h,24h).

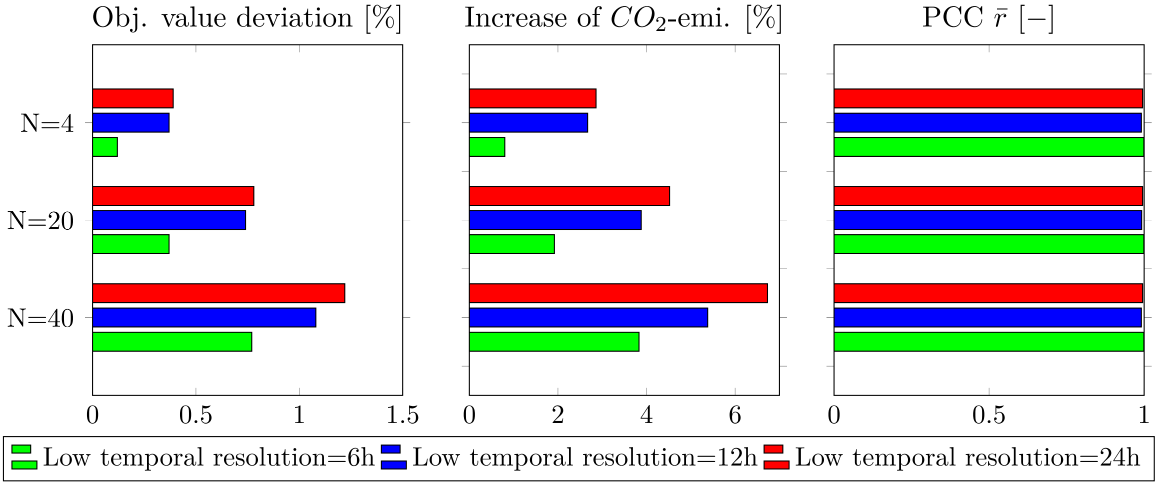

Figure 4.5.: Results of the temporal-hierarchical approach for various temporal resolutions

The figures show two relevant coherencies between the selection of the temporal resolution and the improvement for the RH approach. The first one concerns the chart on the left and the chart in the middle. Both plots show that with the highest temporal resolution of 6h the best results can be achieved compared to the reference model. Furthermore, doubling the temporal resolution leads to a strong increase of the indicators, whereas redoubling the temporal resolution to 24h does not seem to increase the results in a similar way. The second observation concerns the correlation coefficient. Evaluating the chart on the right, the TH approach seems the be very effective in modeling the seasonal storage regardless of the temporal resolution. For each of the resolutions a $\bar{r}$ between 0.991-0.999 is achieved.

In order to answer the question of the most suitable low temporal resolution, two statements derive from the results. First, the improvement of the modeling of seasonal storage seems to be rather independent of the low temporal resolution and delivers a sufficient result for all temporal resolutions. This suggests that even lower temporal resolutions, e.g. 48h, 96h, ..., might be suitable to calculate the necessary supporting points. Hence, the TH approach can be performed with a very low temporal resolution and therefore does not increase the overall computational time in a considerable way. Second, the TH approach does not seem to improve the other indicators in the same manner as $\bar{r}$. Although the previous section showed that an improvement of those indicators can be achieved in comparison to the RH without overlaps, an overlap of 20% or 40% achieves the same results as the TH approach (compare section 4.2.2). In consequence, the use of the TH approach has to be further discussed in the context of a global optimal reduction of the computational time.

## 4.4. Discussion of the results

As an initial step of the analysis of the results, the evaluation of the test model provided a first hypothesis on the dependency of computational-time and the sizing of the RH intervals. The results suggest that there is an optimal number of intervals to achieve a maximum in the reduction of computational time, while other amounts of intervals even lead to an increase of computational time. This hypothesis could be confirmed evaluating the reference model in REMix. Without concerning the use of overlaps, a maximum reduction of computational time of about 50% could be achieved using 8 RH intervals. Therefore, the research question on the possibility of a reduction of computational time can be approved. However a general statement on the best settings of the RH, i.e. choice of number of intervals, cannot be derived of the results as they only apply for the evaluated model size of the reference model.

Further analysis showed that without extending the RH approach with the use of overlaps or a temporal-hierarchical approach, a large error is made in comparison to the results of the reference model. This error mainly derives from the issue of modeling time-integral constraints. The results evaluated in section 4.2 suggest that the use of small overlaps (20%, 40%) is suitable to improve the modeling of time-integral potential limits without a significant increase of computational time. The analysis of the temporal profile of seasonal storage however showed that the use of small overlaps is not sufficient to model the behavior of long term storage. Though, the TH approach is best suited to address that issue using supporting points for the seasonal storage. The TH approach however does not seem to handle the issue of time-integral potential limits for low temporal resolutions of 12h and 24h. Still, acceptable results could be achieved with a temporal resolution of 6h resulting in a total reduction of computational-time of 35%.

Regarding the primary objective of the RH approach of reducing computational time while maintaining a high model quality, a general statement of a preferable approach, i.e. overlap-sizes or TH approach, cannot be made since they both have the mentioned advantages and disadvantages. A combination of both approaches, e.g. a TH approach with a low temporal resolution of 48h combined with a small overlap-size, could deliver the best result in terms of computational time and model quality. The examination of that issue has to be carried out in further analysis.

# 5. Conclusion and Outlook

The intention of this paper was to figure out if and how an implementation of a rolling-horizon approach is suitable to reduce computational-time of large-scale, linear energy system models like REMix while maintaining the key modeling features. The results of the presented work contribute to answer the raised research questions as they implicate the following conclusions:

1. The main challenge regarding the implementation of a RH approach is the precise modeling of time-integral constraints.
2. With regard to the evaluated reference model, the rolling-horizon approach is suitable to reduce computational time by 30-35% without a significant reduction of the modeling quality.
3. The highest reduction of computational time could be achieved using 8 rolling-horizon intervals. Though, a general statement on the optimal number of intervals cannot be derived from the results as they are only valid for the reference model.
4. Referring to 1., the approach of overlap-sizes as well as a the applied temporal-hierarchical approach are able to improve the modeling of time-integral constraints.

A shortcoming of the presented evaluation is that the optimal settings of the RH approach are not transferable to all energy system models. Therefore, the practical application in Energy System Analysis requires further investigation on the dependency of interval-sizing and model reduction time for various model structures and sizes. This analysis aims to develop standard-settings for the RH approach for variable model types.

As the use of overlaps goes along with a strong increase in computational time, the implementation of that approach needs to be improved. This can be achieved through an technique used in [12] which uses a small overlap representing an aggregation of future time steps.

Another improvement of the RH approach can be a parallelization of the solving process. Using the temporal-hierarchical approach, supporting points and potential factors for each interval can be provided. Hence, the intervals can be solved independently of another. Using a parallelizable simulation environment to solve the RH intervals at once promises further acceleration of the computational-time.

Compared to the application of RH approaches in the literature (mostly Mixed-Integer models, e.g. [2]), the presented results are not able to show such a large decrease of computational time (factor 10-100). Regarding the further development of REMix and the extended modeling of power-plants through discrete variables, the RH approach promises a strong impact on the reduction of computational-time for these models.

# Bibliography

[1] Yvonne Scholz. *Renewable energy based electricity supply at low costs: development of the REMix model and application for Europe*. PhD thesis, Universität Stuttgart, 2012.

[2] J. Marquant, R. Elvins, and Carmeliet.J. Reducing computation time with a rolling horizon approach applied to a milp formulation of multiple urban energy hub system. *Procedia Computer Science*, 51:2137 – 2146, 2015.

[3] A. Tuohy, E. Denny, and M. O'Malley. Rolling unit commitment for systems with significant installed wind capacity. In *Power Tech, 2007 IEEE Lausanne*, pages 1380–1385, July 2007.

[4] M. P. Marietta, M. Graells, and J. M. Guerrero. A rolling horizon rescheduling strategy for flexible energy in a microgrid. In *Energy Conference (ENERGYCON), 2014 IEEE International*, pages 1297–1303, May 2014.

[5] N.P. Padhy. Unit Commitment-A Bibliographical Survey. *IEEE Transactions on Power Systems*, 19(2):1196–1205, May 2004.

[6] GAMS Development Corporation. General Algebraic Modeling System (GAMS) Release 24.2.1. Washington, DC, USA, 2013.

[7] Hans Christian Gils. *Balancing of Intermittent Renewable Power Generation by Demand Response and Thermal Energy Storage*. PhD thesis, Universität Stuttgart, 2015.

[8] Karl Kien Cao. Speeding up linear optimization models for energy system analyses - a first performance benchmark of reduction techniques. Research Days 2016, Helmholtz Research School on Energy Scenarios, March 2016.

[9] J. Alemany and F. Magnago. Benders decomposition applied to security constrained unit commitment: Initialization of the algorithm. *International Journal of Electrical Power & Energy Systems*, 66:53 – 66, 2015.

[10] Transpower Stromübertragungs GmbH Vattenfall Europe Transmission GmbH EnBW Transportnetze AG, RWE Transportnetz Strom GmbH. Übersicht über die voraussichtliche Entwicklung der installierten Kraftwerksleistung und der Leistungsflüsse in den Netzgebieten der deutschen übertragungsnetzbetreiber (Regionenmodell Stromtransport 2013), 2009.

[11] Yvonne Scholz, Hans Christian Gils, Thomas Pregger, Dominik Heide, Felix Cebulla, Karl-Kiên Cao, Denis Hess, and Frieder Borggrefe. Möglichkeiten und Grenzen des Lastausgleichs durch Energiespeicher, verschiebbare Lasten und stromgeführte KWK bei hohem Anteil fluktuierender erneuerbarer Stromerzeugung. Technical report, DLR-Institut für Technische Thermodynamik, Juni 2014.

[12] C. Krüger, M. Buddeke, F. Merten, and A. Nebel. Modelling the interdependencies of storage, dsm and grid-extension for europe. In *2015 12th International Conference on the European Energy Market (EEM)*, pages 1–5, May 2015.

[13] IBM. IBM ILOG CPLEX Optimization Studio CPLEX Users Manual V12.6.

[14] Kees Roos, Tamás Terlaky, and Jean-Philippe Vial. *Theory and algorithms for linear optimization / an interior point approach.* Wiley-Interscience series in discrete mathematics and optimization. Wiley, Chichester, repr. edition, 2001.

# A. Appendix

## A.1. Full results of the dispatch model parametr study

Table A.1.: Deviation of the computational-time relative to the reference model [%] for a varying number of intervals and overlap-sizes (entire parameter study)

| Overlap-size [%] | Number of Intervals | | | | | | | | | | | | | |
|---|---|---|---|---|---|---|---|---|---|---|---|---|---|---|
| | 2 | 4 | 6 | 8 | 10 | 20 | 30 | 40 | 50 | 60 | 70 | 80 | 90 | 100 |
| 0 | -30 | -44 | -45 | -47 | -46 | -43 | -35 | -29 | -22 | -12 | -3 | 6 | 13 | 24 |
| 20 | -20 | -35 | -36 | -36 | -36 | -33 | -26 | -22 | -15 | -4 | 4 | 13 | 21 | 29 |
| 40 | -8 | -24 | -27 | -29 | -28 | -25 | -19 | -14 | -8 | 1 | 9 | 18 | 29 | 36 |
| 60 | -4 | -17 | -18 | -22 | -19 | -17 | -14 | -8 | -2 | 9 | 16 | 22 | 33 | 41 |
| 80 | 4 | -4 | -11 | -13 | -14 | -11 | -7 | 0 | 8 | 16 | 22 | 31 | 39 | 48 |
| 100 | 13 | 7 | 1 | -4 | -3 | -2 | 2 | 8 | 14 | 21 | 29 | 38 | 46 | 54 |
| 200 | 87 | 72 | 63 | 55 | 55 | 44 | 48 | 50 | 54 | 61 | 71 | 78 | 83 | 88 |

Table A.2.: Relative deviation of the rolling-horizon objective value to the reference model for a varying number of intervals and overlap-sizes (entire parameter study)

| Overlap-size [%] | Number of intervals | | | | | | | | | | | | | |
|---|---|---|---|---|---|---|---|---|---|---|---|---|---|---|
| | 2 | 4 | 6 | 8 | 10 | 20 | 30 | 40 | 50 | 60 | 70 | 80 | 90 | 100 |
| 0 | 0.13 | 0.98 | 1.02 | 1.03 | 1.48 | 1.69 | 2.30 | 2.76 | 2.90 | 3.19 | 3.33 | 3.57 | 3.68 | 3.87 |
| 20 | 0.09 | 0.06 | 0.24 | 0.28 | 0.32 | 0.59 | 1.02 | 1.17 | 1.46 | 1.54 | 1.80 | 1.87 | 2.15 | 2.07 |
| 40 | 0.10 | 0.05 | 0.07 | 0.10 | 0.12 | 0.28 | 0.47 | 0.64 | 0.78 | 0.81 | 1.07 | 0.99 | 1.23 | 1.34 |
| 60 | 0.03 | 0.04 | 0.06 | 0.08 | 0.10 | 0.21 | 0.34 | 0.52 | 0.54 | 0.58 | 0.74 | 0.65 | 0.84 | 0.95 |
| 80 | 0.02 | 0.04 | 0.05 | 0.07 | 0.09 | 0.19 | 0.30 | 0.38 | 0.56 | 0.61 | 0.60 | 0.69 | 0.84 | 0.84 |
| 100 | 0.02 | 0.03 | 0.05 | 0.06 | 0.07 | 0.18 | 0.28 | 0.30 | 0.48 | 0.54 | 0.57 | 0.62 | 0.77 | 0.63 |
| 200 | 0.01 | 0.03 | 0.03 | 0.04 | 0.05 | 0.09 | 0.18 | 0.21 | 0.25 | 0.37 | 0.41 | 0.43 | 0.53 | 0.50 |

Table A.3.: Mean correlation coefficient $\bar{r}$ for a varying number of intervals and overlap-sizes (entire parameter study)

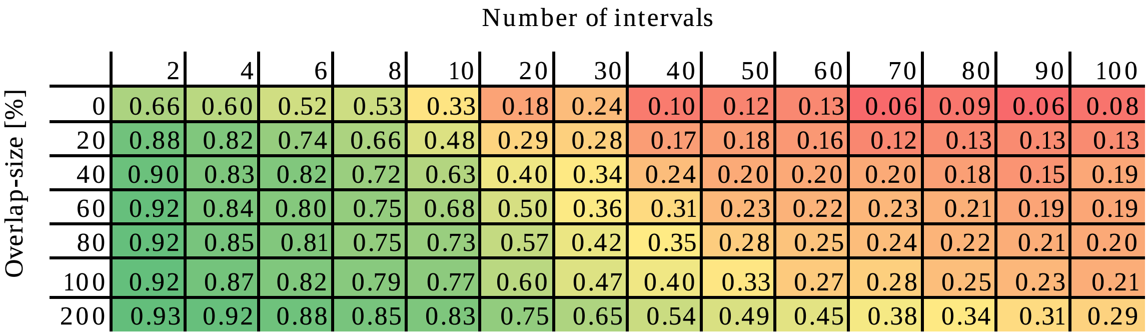

| | Number of intervals | | | | | | | | | | | | | |
|---|---|---|---|---|---|---|---|---|---|---|---|---|---|---|
| Overlap-size [%] | 2 | 4 | 6 | 8 | 10 | 20 | 30 | 40 | 50 | 60 | 70 | 80 | 90 | 100 |
| 0 | 0.66 | 0.60 | 0.52 | 0.53 | 0.33 | 0.18 | 0.24 | 0.10 | 0.12 | 0.13 | 0.06 | 0.09 | 0.06 | 0.08 |
| 20 | 0.88 | 0.82 | 0.74 | 0.66 | 0.48 | 0.29 | 0.28 | 0.17 | 0.18 | 0.16 | 0.12 | 0.13 | 0.13 | 0.13 |
| 40 | 0.90 | 0.83 | 0.82 | 0.72 | 0.63 | 0.40 | 0.34 | 0.24 | 0.20 | 0.20 | 0.20 | 0.18 | 0.15 | 0.19 |
| 60 | 0.92 | 0.84 | 0.80 | 0.75 | 0.68 | 0.50 | 0.36 | 0.31 | 0.23 | 0.22 | 0.23 | 0.21 | 0.19 | 0.19 |
| 80 | 0.92 | 0.85 | 0.81 | 0.75 | 0.73 | 0.57 | 0.42 | 0.35 | 0.28 | 0.25 | 0.24 | 0.22 | 0.21 | 0.20 |
| 100 | 0.92 | 0.87 | 0.82 | 0.79 | 0.77 | 0.60 | 0.47 | 0.40 | 0.33 | 0.27 | 0.28 | 0.25 | 0.23 | 0.21 |
| 200 | 0.93 | 0.92 | 0.88 | 0.85 | 0.83 | 0.75 | 0.65 | 0.54 | 0.49 | 0.45 | 0.38 | 0.34 | 0.31 | 0.29 |

Table A.4.: Increase of carbon emissions [%] for a varying number of intervals and overlap-sizes (entire parameter study)

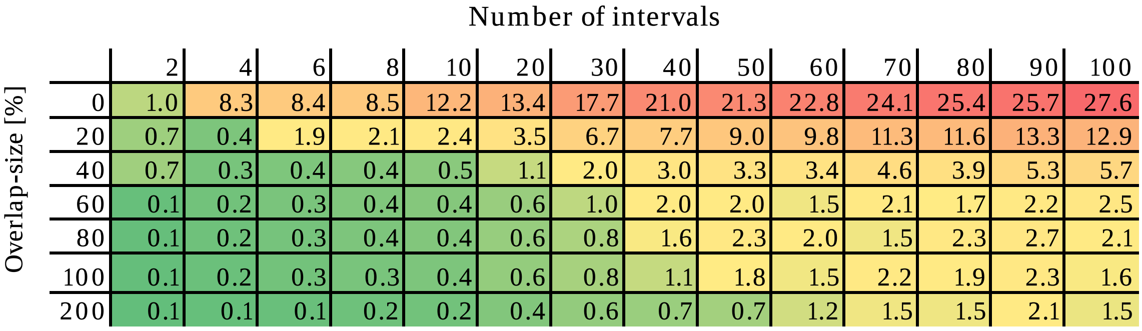

| | Number of intervals | | | | | | | | | | | | | |
|---|---|---|---|---|---|---|---|---|---|---|---|---|---|---|
| Overlap-size [%] | 2 | 4 | 6 | 8 | 10 | 20 | 30 | 40 | 50 | 60 | 70 | 80 | 90 | 100 |
| 0 | 1.0 | 8.3 | 8.4 | 8.5 | 12.2 | 13.4 | 17.7 | 21.0 | 21.3 | 22.8 | 24.1 | 25.4 | 25.7 | 27.6 |
| 20 | 0.7 | 0.4 | 1.9 | 2.1 | 2.4 | 3.5 | 6.7 | 7.7 | 9.0 | 9.8 | 11.3 | 11.6 | 13.3 | 12.9 |
| 40 | 0.7 | 0.3 | 0.4 | 0.4 | 0.5 | 1.1 | 2.0 | 3.0 | 3.3 | 3.4 | 4.6 | 3.9 | 5.3 | 5.7 |
| 60 | 0.1 | 0.2 | 0.3 | 0.4 | 0.4 | 0.6 | 1.0 | 2.0 | 2.0 | 1.5 | 2.1 | 1.7 | 2.2 | 2.5 |
| 80 | 0.1 | 0.2 | 0.3 | 0.4 | 0.4 | 0.6 | 0.8 | 1.6 | 2.3 | 2.0 | 1.5 | 2.3 | 2.7 | 2.1 |
| 100 | 0.1 | 0.2 | 0.3 | 0.3 | 0.4 | 0.6 | 0.8 | 1.1 | 1.8 | 1.5 | 2.2 | 1.9 | 2.3 | 1.6 |
| 200 | 0.1 | 0.1 | 0.1 | 0.2 | 0.2 | 0.4 | 0.6 | 0.7 | 0.7 | 1.2 | 1.5 | 1.5 | 2.1 | 1.5 |